Molecular Therapy
Oncology
Original Article

Antigen-binding affinity is a key determinant of the durable antitumor activity of CD5 CAR-T cells

Jeong-Hoon Jeong,[1] Yu Ri Seo,[1] Seung Rok Yu,[1] Hyo Bhin Lee,[1] Hyeong Ji Lee,[1] Hyeon Jeong Cho,[1] Hyung Cheol Kim,[1] and Young-Ho Lee[1]

[1]Curocell Inc., Daejeon 34002, Republic of Korea

T cell fratricide in T cell antigen-targeted chimeric antigen receptor (CAR)-T cell therapies remains a critical barrier to achieving optimal antitumor efficacy. To address this challenge, we explored modulation of antigen-binding affinity as a simple yet effective strategy to mitigate fratricide. To this end, we aimed to develop low-affinity CD5-specific CAR-T cells and to test the hypothesis that low-affinity CD5 CAR-T cells can evade T cell fratricide, thereby alleviating T cell exhaustion and enhancing sustained antitumor activity. Our results demonstrate that CD5 CAR-T cells engineered with low-affinity monoclonal antibodies exhibit significantly reduced fratricide and diminished T cell exhaustion in the infusion product compared to high-affinity counterparts such as the standard H65 and A2 clones, which is assumed to correlate with improved long-term antitumor responses. These findings establish antigen-binding affinity modulation as a promising alternative to extensive gene editing approaches, potentially simplifying CD5 CAR-T cell manufacturing while improving therapeutic outcomes.

INTRODUCTION

T cell lymphomas, including T cell acute lymphoblastic leukemia (T-ALL) and peripheral T cell lymphoma, continue to represent a significant therapeutic challenge due to their aggressive clinical behavior and suboptimal response to conventional chemotherapies.[1,2] Standard regimens often result in high relapse rates and poor long-term survival, underscoring the urgent need for innovative therapeutic approaches. Targeted agents such as mogamulizumab and brentuximab vedotin have shown some efficacy, but their impact is limited by resistance, toxicities, and restricted applicability to specific patient subgroups.[3–6] In recent years, adoptive immunotherapy—particularly chimeric antigen receptor (CAR)-T cell therapy—has emerged as a promising modality for achieving favorable clinical outcomes in the treatment of T cell malignancies.[7,8] However, the application of CAR-T cells in T cell malignancies is uniquely hindered by tumor contamination and CAR-T cell fratricide.[9–11] CAR-T cell fratricide occurs when CAR-T cells attack each other due to shared T cell antigens, including CD5, CD7, and CD30, leading to premature CAR-T cell exhaustion and ultimately compromising therapeutic efficacy.[12–15] Thus, for CAR-T therapies targeting T cell antigens, it is critical to adopt strategies that mitigate fratricide.

To address these limitations, recent efforts have primarily focused on using CRISPR-Cas9 gene editing to eliminate T cell antigen expression and thereby prevent T cell fratricide.[12,14,16,17] While knockout strategies can be effective, they require extensive genetic modifications that complicate the manufacturing process and may inadvertently affect T cell functions. Moreover, CRISPR-Cas9-induced chromosomal abnormalities, notably chromosome loss, pose safety concerns for engineered T cell therapies.[18–20] While base editing offers a less mutation-prone alternative,[21] we sought to avoid CAR-T fratricide by tuning antigen-binding affinity, thereby eliminating the need for additional genetic modifications altogether.

It is well established that the affinity of the antigen-binding domain in CAR-T cells can influence T cell activation and subsequent antitumor responses.[22,23] Traditionally, high-affinity antigen-binding domains have been favored due to their ability to induce robust activation and detect low levels of antigen, as exemplified by the FMC63 monoclonal antibody used in CD19 CAR-T cells (KD = 0.32 nM).[24–26] However, excessively high-affinity interactions with target antigens—especially when the target is also expressed on normal T cells—may lead to adverse outcomes such as tonic signaling, chronic activation, and CAR downregulation via trogocytosis, ultimately contributing to T cell exhaustion and reduced therapeutic efficacy.[27] These limitations have prompted growing interest in low-affinity CARs, which have demonstrated improved persistence and reduced dysfunction in preclinical models targeting antigens such as CD19 and CD229.[24,28] These findings suggest that modulating antigen-binding affinity could be a broadly applicable strategy to optimize CAR-T cell performance.

Received 5 August 2025; accepted 12 February 2026;
https://doi.org/10.1016/j.omton.2026.201158.

Correspondence: Young-Ho Lee, Curocell Inc., Daejeon 34002, Republic of Korea.
E-mail: yhlee@curocellbtx.com

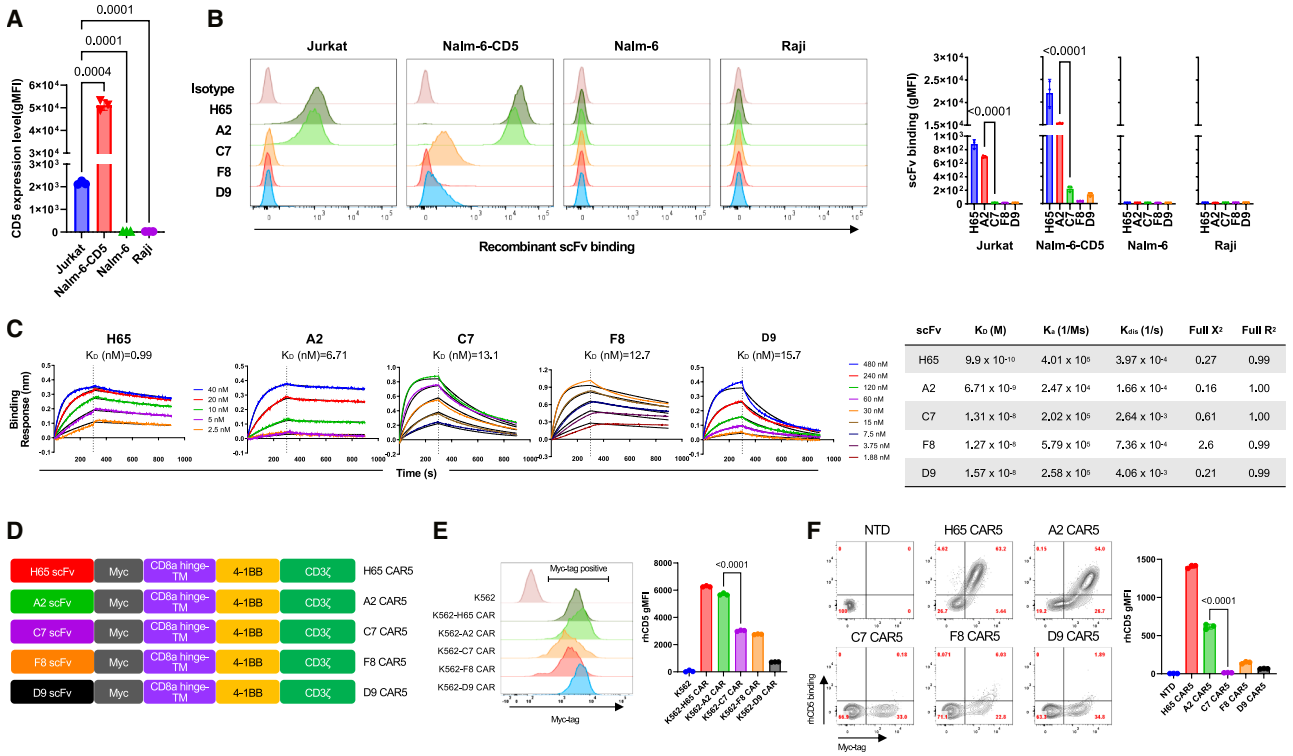

Figure 1. Generation and characterization of CD5 CAR-T cells with distinct binding affinities

(A) CD5 expression levels of various cell lines, including T cell leukemia cell line (Jurkat), as assessed by flow cytometry. Data are presented as mean ± SD from technical replicates ($n = 3$). (B) Binding of recombinant anti-CD5 scFvs to CD5-positive and CD5-negative cell lines as measured by flow cytometry. Gray indicates the isotype control. Numbers represent geometric mean fluorescence intensity (gMFI). Data are presented as mean ± SD from technical replicates ($n = 3$). (C) Affinity properties of anti-CD5 scFvs as determined by biolayer interferometry using Octet system. H65 scFv was used as a positive control scFv. KD, equilibrium dissociation constant; K_a, association rate constant; K_{dis} (1/s), dissociation rate constant. Full X^2, sum of squared deviations; values near zero indicate a good curve fit. Full R^2, coefficient of determination; values near 1.0 indicate a good curve fit. $R^2 < 0.98$ or $X^2 > 3$ was considered unreliable. (D) Schematic illustration of a lentiviral vector encoding anti-CD5 CAR constructs with Myc tag. Colors denote scFv origin: red for H65, green for A2, purple for C7, orange for F8, and black for D9. (E) Surface CAR expression of each K562-CAR cell line was analyzed with anti-Myc-tag antibody and recombinant human CD5 (rhCD5). Data are presented as mean ± SD from technical replicates ($n = 3$). (F) Surface CAR expression of each CAR-T cell product was assessed by anti-Myc-tag antibody and rhCD5 binding on day 3 after cell seeding. Data are presented as mean ± SD from multiple donors ($n = 3$). Statistical analyses were performed using one-way ANOVA with Tukey's multiple comparisons test for (A, B, and E) and a linear mixed-effects model with donor as a random effect followed by Tukey's test for (F).

Here, we hypothesized that lowering the antigen-binding affinity of CD5 CAR-T cells could mitigate fratricide and reduce T cell exhaustion, ultimately enhancing antitumor efficacy. To test this hypothesis, we screened human anti-CD5 monoclonal antibodies with varying affinities and evaluated their effects on CAR-T cell exhaustion, fratricide, and therapeutic efficacy. Additionally, to minimize the influence of other scFv-intrinsic properties, we fine-tuned CAR affinity through alanine scanning and random mutagenesis of the scFv complementarity-determining regions (CDRs) and assessed the resulting exhaustion and fratricide levels. Our findings demonstrate that antigen-binding affinity critically influences fratricide and exhaustion in CD5 CAR-T cells, suggesting affinity modulation as a simpler alternative to gene editing for fratricide prevention—potentially streamlining CAR-T manufacturing and improving therapeutic efficacy.

RESULTS

Characterization of novel human CD5-specific monoclonal antibodies and generation of CD5-specific CAR-T cells

To elucidate the effect of antigen-binding affinity on fratricide and exhaustion in T cell antigen-targeting CAR-T cells, we first screened novel human monoclonal antibodies specific for CD5. Using phage display, we successfully found and identified four novel human monoclonal antibodies specific for CD5 with the distinct amino acid sequence of their heavy chain CDRs.

Subsequently, to evaluate antigen specificity, we first assessed CD5 expression across multiple cell lines by flow cytometry (Figure 1A), followed by cellular-binding assays using recombinant anti-CD5 scFvs (Figure 1B). While all scFvs bound to recombinant human CD5 (rhCD5), their ability to recognize cell surface CD5 varied considerably. Specifically, the H65 clone, representative anti-CD5

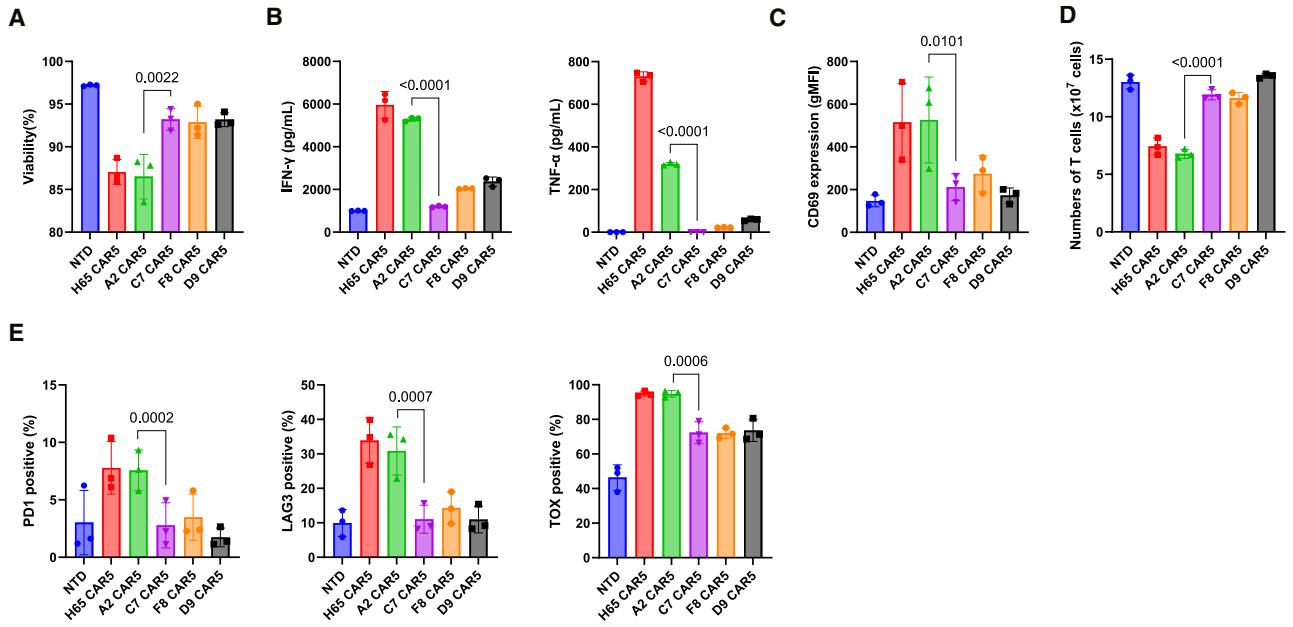

Figure 2. Low-affinity CD5 CAR-T cells exhibit reduced fratricide and exhaustion phenotypes

(A) Viability of CAR-T cells measured on day 3 after cell seeding. Data are presented as mean ± SD from multiple donors ($n = 3$). (B) Culture supernatants were collected on day 3 after cell seeding. IFN-γ and TNF-α levels secreted by CAR -T cells were measured by cytometric bead array. Data are presented as mean ± SD from multiple donors ($n = 3$). (C) CD69 expression level of CAR-T cells on day 10 after seeding. Fluorescence intensity was quantified by flow cytometry. Data are presented as mean ± SD from multiple donors ($n = 3$). (D) Total T cell number harvested on day 10 after cell seeding. Data are presented as mean ± SD from multiple donors ($n = 3$). (E) Expression levels of PD-1 and LAG-3 (surface markers), and TOX (intracellular marker) in CAR-T cells on day 10 after seeding. Surface markers were analyzed by flow cytometry, and TOX expression was assessed via intracellular staining following fixation and permeabilization. Data are presented as mean ± SD from multiple donors ($n = 3$). All statistical significance was assessed using a linear mixed-effects model with donor as a random effect and Tukey's test.

antibody,[8] and our novel A2 clone exhibited strong binding to Jurkat and Nalm-6-CD5 cells, both of which express CD5, but showed no binding to Raji and parental Nalm-6 cells, lacking CD5 expression. In contrast, clones C7, F8, and D9 retained specificity for CD5 but displayed markedly weaker binding to cell-surface CD5.

We further quantified the binding affinity (K_D) of each antibody clone using a biolayer interferometry (BLI) (Figure 1C). The affinities ranged from 0.99 to 15.7 nM, with H65 and A2 clones exhibiting higher binding affinities than C7, F8, and D9. More specifically, while the association constants (K_a) were comparable across all antibodies, the dissociation constants (K_{dis}) of C7 and D9 were significantly lower than those of H65 and A2. These results indicate a close correlation between the binding profiles observed in cellular-binding assays and the measured antibody affinities.

Next, we engineered second-generation CAR constructs incorporating the 4-1BB co-stimulatory domain for each clone (Figure 1D). To ensure clinical relevance, we included the H65-based CAR (H65-BBz) as a high-affinity benchmark, representing the current clinical-stage CD5 CAR-T therapy.[8] We first confirmed that the CARs derived from each clone were stably expressed and preserved the inherent antigen-binding affinities in CD5-negative K562 cells (Figure 1E). Furthermore, CAR-T cells were generated using all five CAR constructs, each exhibiting their antigen-binding intensities (Figure 1F). In summary, these results demonstrate the successful development of a panel of CAR-T cells with varying binding affinities, providing a robust model to investigate the impact of antigen-binding strength on the phenotype and function of T cell antigen-targeting CAR-T cells.

Low-affinity CD5 CAR-T cells exhibit a less fratricidal and exhausted phenotype

To investigate the impact of CAR affinity on fratricide and exhaustion in CD5 CAR-T cells, we first evaluated the fratricidal phenotype during manufacturing by assessing cell viability, cell expansion, cytokine secretion, and activation status. Our results showed that, following CAR transduction, a marked increase in cell death and cytokine secretion was observed beginning on day 3, indicative of the onset of fratricide (Figures 2A and 2B). These were especially prominent in CD5 CAR-T cells generated using high-affinity clones (H65 and A2 CAR-T cells), which showed significantly elevated levels of both cell death and proinflammatory cytokine production compared to those generated with low-affinity clones (C7, F8, and D9 CAR-T cells). Furthermore, on day 10, when CAR-T cell manufacturing was completed, H65 and A2 CAR-T cells remained highly activated (Figure 2C) and the number of T cells obtained (Figure 2D) was lower compared to the other CAR-T cell products.

Taken together, these findings indicate that H65 and A2 CAR-T cells undergo substantially higher levels of fratricide than their low-affinity counterparts. We next evaluated the expression of exhaustion-associated markers such as PD-1, LAG-3, and TOX and found that low-affinity CAR-T cells demonstrated a less-exhausted phenotype compared to their high-affinity counterparts (Figure 2E). In summary, these data suggest that the affinity of the antigen-binding domain can influence the strength of CAR signaling, thereby promoting a more fratricidal and exhausted CAR-T cell phenotype.

CAR affinity controls fratricide and exhaustion CD5 CAR-T cells

Each anti-CD5 scFv exhibits distinct properties, including structural stability and binding epitope, which may influence the extent of fratricide when used in CAR-T cell manufacturing and potentially confound interpretation. To address this, we generated A2 and C7 variants with altered binding affinity using site-directed and random mutagenesis, respectively, to rigorously investigate the impact of affinity on fratricide and exhaustion in CD5 CAR-T cells.

We first performed alanine scanning of the A2 clone by substituting each amino acid in the heavy chain CDR3 region with alanine, generating nine A2 CAR variants (Figure S1A), which were transduced into K562 cells (Figure S1B). To identify variants with the weakest antigen-binding strength, we assessed their binding to recombinant human CD5 (rhCD5) and selected the three variants with the lowest binding levels—D1A, W2A, and Y4A—compared to the wild-type (Figure S1C). Their antigen specificity and binding properties of antibodies were also determined through a cellular binding assay (Figure 3A). We further quantified the binding affinity (K_D) of each variant (Figure 3B). The D1A and W2A variants exhibited K_D values of 30.9 and 7.67 nM, respectively, both of which were lower than that of the A2 wild-type. Y4A showed binding that was too weak to be reliably quantified.

We next examined phenotypic changes in CD5 CAR-T cells expressing these variants. Compared to A2 wild-type CAR5 cells, both W2A and Y4A CAR5 cells exhibited reduced cell death and decreased cytokine secretion during culture (Figures 3C and 3D). Additionally, total T cell yield was higher, and the activation state was significantly lower in these variants at day 10 (Figures 3E and 3F). Expression of exhaustion-associated markers was also markedly decreased in W2A and Y4A CAR5 cells (Figure 3G). In serial rechallenge assays at an effector-to-target (E:T) ratio of 3:1, low-affinity CAR-T cells (C7 and Y4A) sustained their proliferative capacity (Figure 3H) while achieving effective tumor control (Figure S2). These cells maintained low expression of exhaustion markers during manufacturing (Figure 3G), preserving their functional fitness. In contrast, high-affinity A2 CAR-T cells, which exhibited elevated exhaustion markers during manufacturing (Figure 3G), showed diminished expansion upon rechallenge (Figures 3H and S2).

To complement this approach, we introduced random mutations into the heavy chain CDR3 region of the C7 clone, exhibiting weak affinity to CD5 and performed biopanning to isolate higher-affinity variants. This strategy yielded the S6E (ES) and S6E/S7E (EE) clones, both of which displayed increased binding affinities compared to the C7 wild-type (Figures 4A and 4B). We generated CAR5 constructs incorporating C7 variants (S6E CAR5 and S6E/S7E CAR5) and evaluated their phenotype. S6E CAR5 and S6E/S7E CAR5 showed significantly increased cell death and cytokine secretion (Figures 4C and 4D) as well as higher activation and reduced T cells yields at day 10 (Figures 4E and 4F). In addition, both variants showed increased expression of exhaustion-associated markers, including immune checkpoint receptors and TOX (Figure 4G), and their proliferative capacity upon repeated antigen stimulation was markedly diminished (Figures 4H and S2).

These results indicate that the affinity-enhanced C7 variants exhibit increased fratricide and exhaustion compared to the C7 wild-type CAR5.

Collectively, these complementary models—affinity attenuation of A2 and enhancement of C7—demonstrate that CAR antigen-binding affinity is a critical determinant of fratricide and exhaustion in CD5 CAR-T cells.

Low-affinity CD5 CAR-T cells exhibit enhanced antitumor activity and prolonged *in vivo* persistence

To elucidate the impact of antigen-binding affinity of CD5-targeting CARs on their functional capacity, we first performed *in vitro* cytotoxicity assays using several CD5-positive T cell lines (Jurkat, HUT78, PRMI8402, and CCRF-CEM) that represent a spectrum of CD5 antigen densities (Figure S3). High-affinity CAR-T cells (A2 and H65 CAR5) exhibited significantly greater cytotoxicity and interferon (IFN)-γ secretion than their counterparts (C7, F8, and D9 CAR5) (Figures 5A, 5B, and S4).

Notably, while low-affinity clones exhibited minimal cytokine production against endogenous T cell lines at standard ratios, we investigated whether they retained the functional capacity to respond to stronger antigenic stimulation. To validate their functional integrity, we challenged these CAR-T cells with Nalm6-CD5 cells, which express approximately 25-fold higher CD5 levels than Jurkat cells (Figure 1A). Against this high antigen-density target, C7 CAR5 demonstrated robust and significant secretion of both IFN-γ and tumor necrosis factor (TNF)-α (Figure S5). These results demonstrate that low-affinity CARs retain intrinsic capacity for antigen-specific activation, which is effectively triggered once the antigenic stimulus surpasses their specific activation threshold.

Next, we evaluated antitumor efficacy in a T-ALL xenograft model. Given that antigen density is a critical determinant of CAR-T efficacy, we prioritized Jurkat cells as the primary *in vivo* model. This selection ensured a rigorous assessment of physiological CD5 levels, as Jurkat cells exhibit the lowest antigen expression among the tested T cell cancer lines (Figure S3). Accordingly, NOG mice were intravenously engrafted with firefly luciferase-expressing Jurkat cells, followed by CAR-T infusion on day 7. Tumor progression was

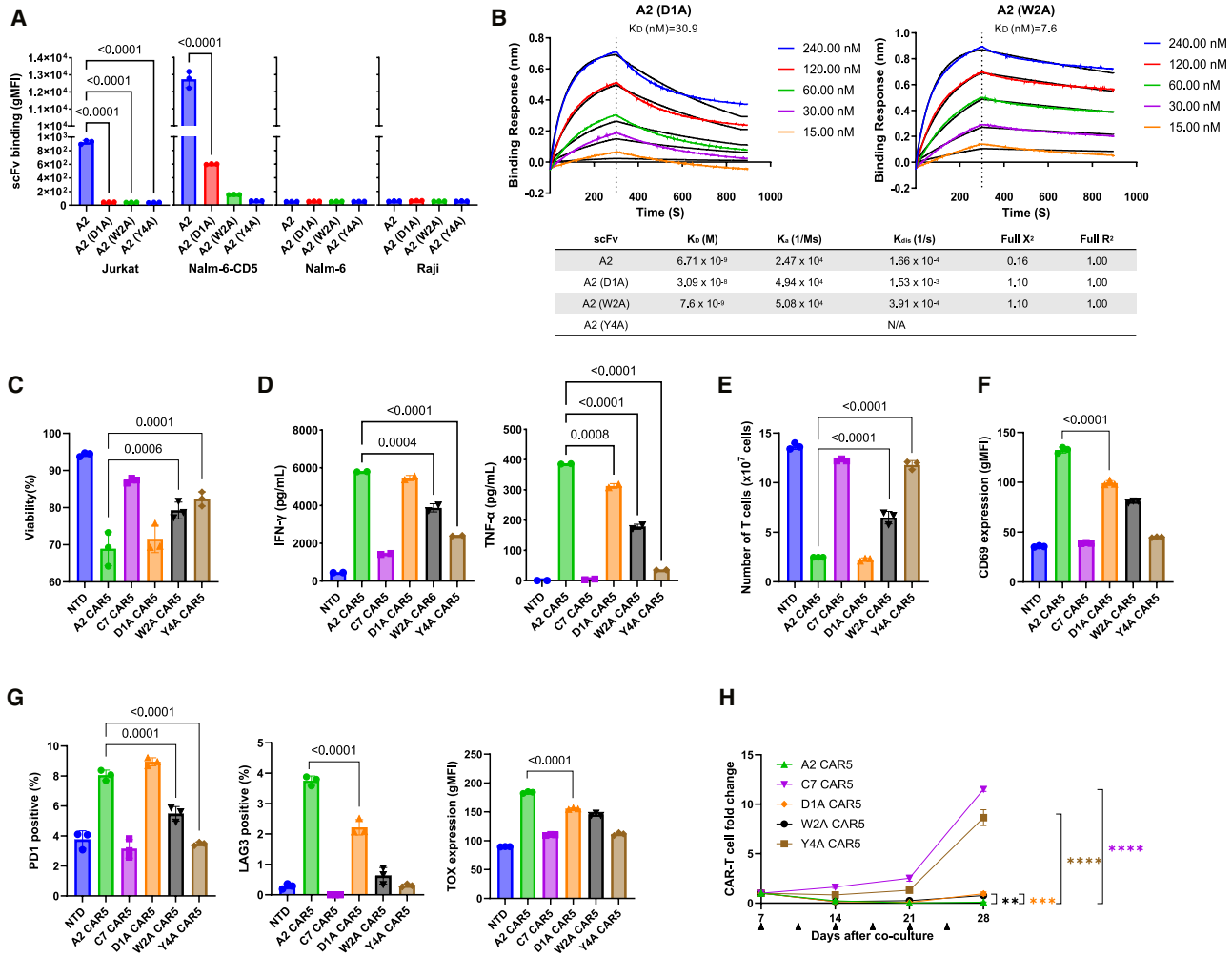

Figure 3. Affinity-tuned A2 variants provide functional evidence that antigen-binding affinity plays a key role in regulating fratricide and T cell exhaustion

(A) Binding level of recombinant anti-CD5 scFvs to CD5-positive and CD5-negative cell lines, as measured by flow cytometry. Data are presented as mean ± SD from technical replicates (n = 3). (B) Affinity properties of anti-CD5 scFvs as determined by biolayer interferometry using Octet system. A2 scFv was used as controls. (For definitions of K_D, K_a, K_{dis}, and curve fit parameters, refer to Figure 1 legend.) (C) Viability of CAR-T cells measured on day 3 after cell seeding. Data are presented as mean ± SD from multiple donors (n = 3). (D) Culture supernatants were collected on day 3 to assess IFN-γ and TNF-α secretion, measured using cytometric bead array. Data are presented as mean ± SD from technical replicates (n = 3). (E) Total T cell number harvested on day 10 after cell seeding. Data are presented as mean ± SD from multiple donors (n = 3). (F) CD69 expression levels in CAR-T cells on day 10 after cell seeding, measured by surface staining and flow cytometry. Data are presented as mean ± SD from multiple donors (n = 3). (G) Expression levels of PD-1 and LAG-3 (surface markers) and TOX (intracellular) in CAR-T cells on day 10 after seeding. Surface markers were analyzed by flow cytometry, and TOX expression was assessed via intracellular staining. Data are presented as mean ± SD from multiple donors (n = 3). (H) 3×10^5 Myc$^+$ CAR-T cells were co-cultured with 1×10^5 Jurkat cells every 3–4 days for repeated antigen stimulation. Expansion of Myc$^+$ CAR-T cells was measured weekly by flow cytometry. Data are presented as mean ± SD from technical replicates (n = 3). Statistical analyses were performed using one-way ANOVA with Tukey's multiple comparisons test for (A, D, and H) and a linear mixed-effects model with donor as a random effect followed by Tukey's test for (C–G).

monitored weekly for 26 days using bioluminescence imaging. Low-affinity CAR-T groups demonstrated superior tumor control compared to high-affinity CAR-T groups (Figure 5C). In contrast, mice treated with high-affinity CAR-T cells showed earlier loss of tumor control.

To determine whether the observed differences in antitumor activity between the two groups were associated with *in vivo* expansion, we quantified circulating CAR-T cells on days 3, 7, 15, and 21 post-infusion. C7 CAR5 cells exhibited robust expansion, peaking at levels approximately 22.7-fold higher than A2 CAR5 cells, and persisted in the blood for up to 3 weeks. In contrast, A2 CAR5 showed minimal expansion across all time points. (Figure 5D). Consistent with these observations, mice treated with C7 CAR5 exhibited improved survival (Figure 5E).

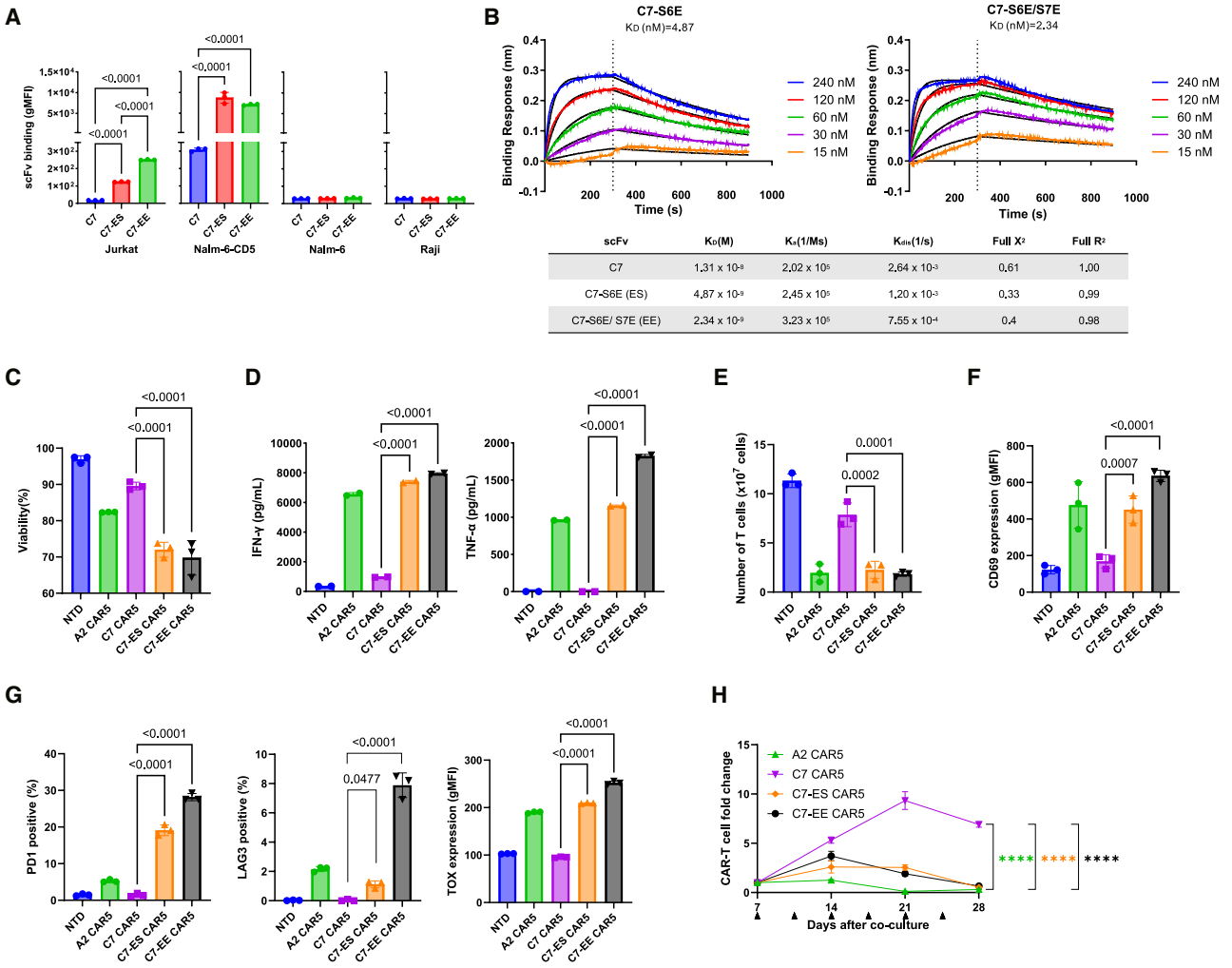

scFv	K_D(M)	K_a(1/Ms)	K_{dis}(1/s)	Full X^2	Full R^2
C7	1.31 x 10^{-8}	2.02 x 10^5	2.64 x 10^{-3}	0.61	1.00
C7-S6E (ES)	4.87 x 10^{-9}	2.45 x 10^5	1.20 x 10^{-3}	0.33	0.99
C7-S6E/ S7E (EE)	2.34 x 10^{-9}	3.23 x 10^5	7.55 x 10^{-4}	0.4	0.98

Figure 4. High-affinity C7 variant-based CAR5 exhibited increased levels of both fratricide and T cell exhaustion compared to the C7 wild-type CAR5

(A) Binding level recombinant anti-CD5 scFvs to CD5-positive and CD5-negative cell lines, as measured by flow cytometry. Data are presented as pooled mean ± SD from technical replicates (n = 3). (B) Affinity properties of anti-CD5 scFvs as determined by biolayer interferometry using Octet system. C7 scFv was used as controls. (For definitions of K_D, K_a, K_{dis}, and curve fit parameters, refer to Figure 1 legend.) (C) Viability of CAR-T cells measured on day 3 after cell seeding. Data are presented as mean ± SD from multiple donors (n = 3). (D) Culture supernatants were collected on day 3 to assess IFN-γ and TNF-α secretion, measured using cytometric bead array. Data are presented as mean ± SD from technical replicates (n = 3). (E) Total T cell number harvested on day 10 after cell seeding. Data are presented as mean ± SD from multiple donors (n = 3). (F) CD69 expression levels in CAR-T cells on day 10 after cell seeding, measured by surface staining and flow cytometry. Data are presented as mean ± SD from multiple donors (n = 3). (G) Expression levels of PD-1 and LAG-3 (surface markers) and TOX (intracellular) in CAR-T cells on day 10 after seeding. Surface markers were analyzed by flow cytometry, and TOX expression was assessed via intracellular staining. Data are presented as mean ± SD from multiple donors (n = 3). (H) 3 × 10^5 Myc^+ CAR-T cells were co-cultured with 1 × 10^5 Jurkat cells every 3–4 days for repeated antigen stimulation. Expansion of Myc^+ CAR-T cells was measured weekly by flow cytometry. Data are presented as mean ± SD from technical replicates (n = 3). Statistical analyses were performed using one-way ANOVA with Tukey's multiple comparisons test for (A, D, and H) and a linear mixed-effects model with donor as a random effect followed by Tukey's test for (C–G).

In summary, our findings demonstrate that the antigen-binding affinity of CAR5 critically influences the *in vivo* antitumor efficacy of CD5-targeting CAR-T cells.

Allogeneic CD5 CAR γδ T cells with low-affinity exhibit enhanced antitumor responses

The significant concern of tumor contamination by patient-derived T cells underscores the necessity for developing allogeneic, blast-free CAR-T therapies for T cell lymphoma. Healthy donor-derived γδ T cells are particularly attractive candidates for allogeneic CAR-T therapy due to their inherently blast-free nature and minimal risk of inducing graft-versus-host disease (GvHD). They also represent a T cell subset with lower baseline CD5 expression compared to αβ T cells[29,30] (Figure S6), a feature that may further reduce the risk of fratricide. With this rationale, we developed an anti-CD5 γδ CAR-T cell (γδCAR5) and evaluated whether modulating the

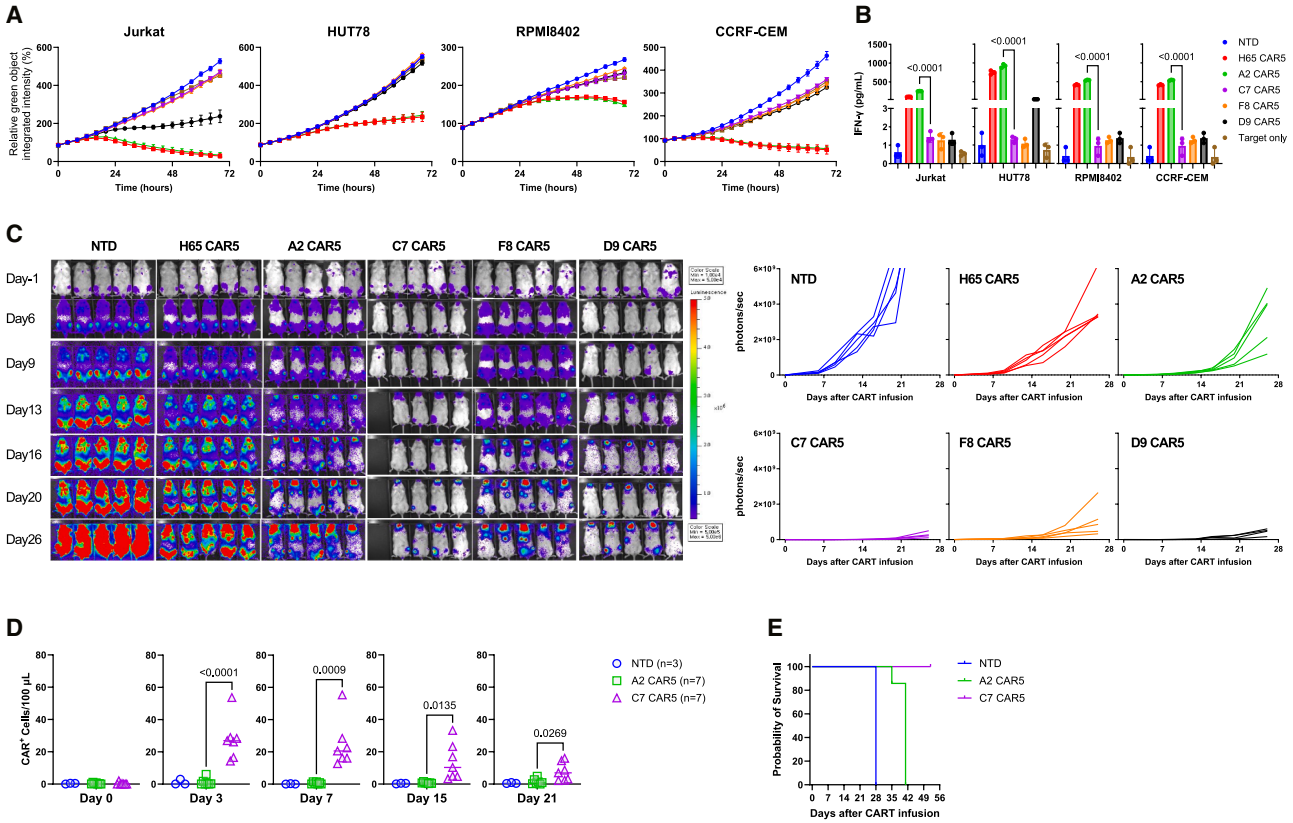

Figure 5. Low-affinity CAR-T cells demonstrate superior *in vivo* antitumor activity despite reduced immediate cytotoxicity

(A) CAR-T cells were co-cultured with ZsGreen-expressing T cell lymphoma cell lines (Jurkat, HUT78, RPMI8402, and CCRF-CEM) at a 1:1 E:T ratio. GFP intensity was measured every 4 h using the IncuCyte S3 live-cell imaging system. Relative total integrated GFP intensity was calculated as [GFP intensity at each time point ÷ GFP intensity at 4 h] × 100. Data are presented as mean ± SD from technical replicates ($n = 3$). (B) IFN-γ and TNF-α levels secreted by CD5 CAR-T cells co-cultured with T cell malignancy-derived cell lines for 3 days at a 1:1 E:T ratio. Data are presented as mean ± SD from technical replicates ($n = 3$). (C) NOG mice were intravenously injected with 1×10^6 Jurkat-GL cells. 7 days later, 1×10^6 CAR-T cells were administered intravenously. Tumor burden was monitored by bioluminescence imaging using the IVIS Lumina system. Data represent $n = 5$ for both NTD and CAR5 groups. (D) NOG mice were intravenously injected with 1×10^6 Jurkat-GL cells. 7 days later, 4×10^6 CAR-T cells were administered. CAR-T cell kinetics in peripheral blood was assessed by flow cytometry with Absolute Counting Beads. Data represent $n = 3$ for NTD and $n = 7$ for CAR5 groups. (E) Kaplan-Meier survival curves for mice described in (D). Statistical analyses were performed using one-way ANOVA with Tukey's multiple comparisons test for (B and D) and log rank (Mantel-Cox) test for (E).

antigen-binding affinity of CD5-targeting CARs could enhance its antitumor activity.

To generate γδCAR5, we transduced Vγ9Vδ2-enriched T cells with either A2 CAR5 or C7 CAR5 (Figure 6A). We first confirmed that over 90% of the γδCAR5 cells expressed the Vδ2 TCR, indicating successful enrichment of Vγ9Vδ2 T cells (Figure 6B). Both A2 CAR5 and C7 CAR5 were robustly expressed on the surface of γδ T cells (Figure 6C). Next, we assessed whether the affinity of CAR5 influences T cell fratricide and exhaustion in γδCAR5 cells. Consistent with our findings in αβCAR5, C7 γδCAR5 cells exhibited significantly lower cytokine secretion and CD69 expression (Figure 6D). Additionally, the percentages of LAG-3^+ cells, TIM-3^+ cells, and TOX expression were lower in C7 γδCAR5, indicating reduced expression of exhaustion-associated markers (Figure 6E).

We then evaluated antitumor efficacy in xenograft model of T-ALL. Firefly luciferase-expressing Jurkat cells were intravenously engrafted into NOG mice, followed by infusion of CAR-T cells on day 7. As expected, C7 γδCAR5 cells demonstrated superior antitumor activity compared to A2 γδCAR5 cells (Figure 6F). Moreover, C7 γδCAR5 cells expanded more robustly *in vivo*, peaking at day 3 at a level approximately 3-fold higher than A2 γδCAR5 cells (Figure 6G). This enhanced expansion ultimately translated into prolonged survival in the C7 γδCAR5 group (Figure 6H).

In summary, our results demonstrate that modulating antigen-binding avidity enhances the antitumor activity of allogeneic γδ CAR-T cells against T cell malignancies, implying that avidity tuning represents a universal and broadly applicable strategy for optimizing the efficacy of all engineered immune cell therapies targeting T cells.

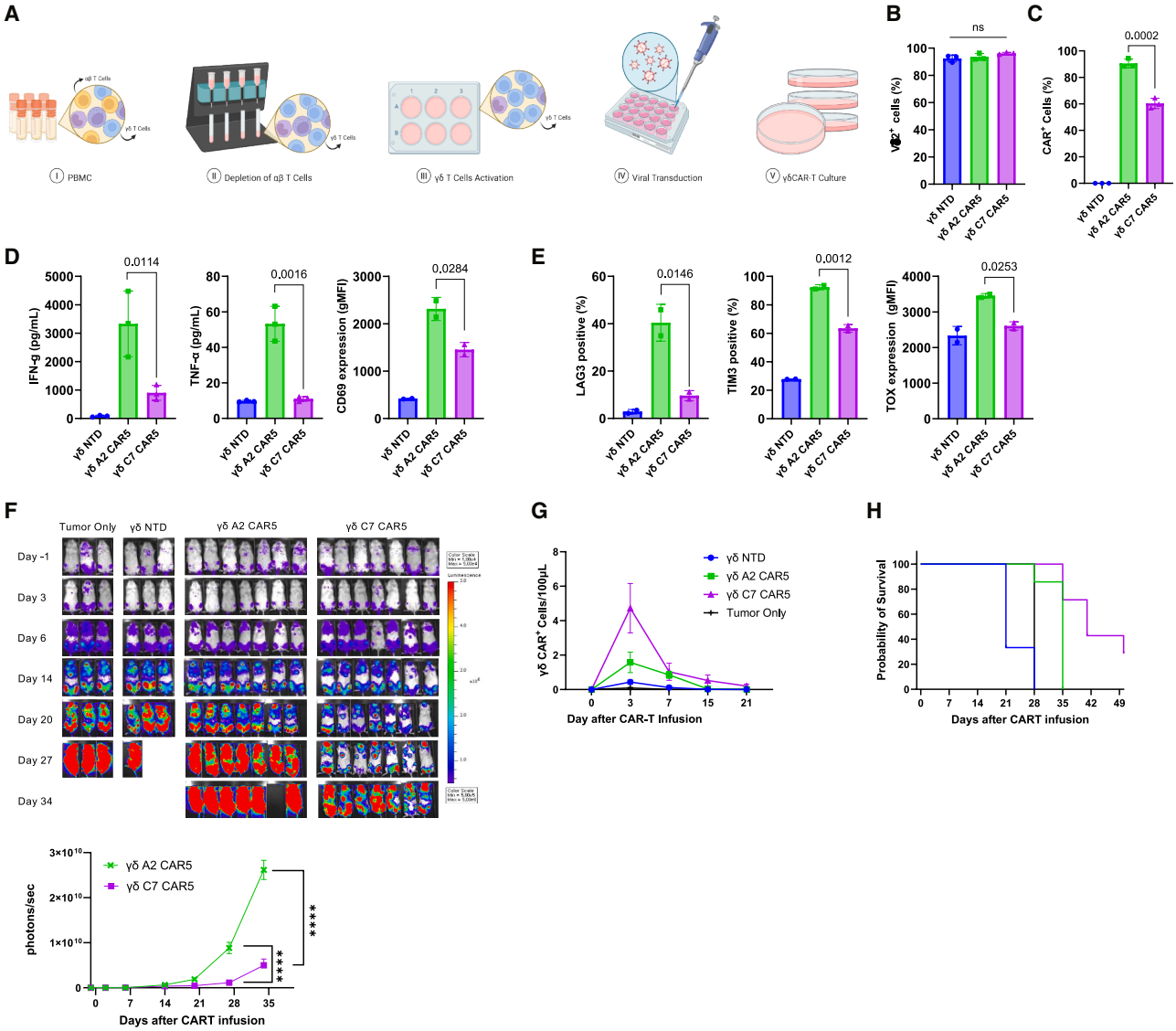

Figure 6. Low-affinity anti-CD5 CAR enhances functional persistence and antitumor activity in γδ CAR5 cells

(A) Schematic overview of the generation process for γδ CAR-T cells (B) Proportion of Vδ2-positive cells among γδ T cells after CAR transduction, as assessed by flow cytometry. Data are presented as mean ± SD from multiple donors (n = 3). (C) Percentage of CAR-expressing cells within the γδ T cell population on day 10, determined by staining with anti-Myc antibody. Data are presented as mean ± SD from multiple donors (n = 3). (D) IFN-γ and TNF-α levels secreted by CAR-T on day 3 of culture, measured by cytometric bead array. CD69 surface expression was analyzed by flow cytometry on day 10. Data are presented as mean ± SD from multiple donors (n = 3). (E) Expression levels of LAG-3 and TIM-3 (surface markers) and TOX (intracellular marker) in γδ CAR-T cells on day 10. TOX expression was assessed by intracellular staining after fixation/permeabilization. Data are presented as mean ± SD from multiple donors (n = 2). (F) NOG mice were intravenously injected with 1×10^6 Jurkat-GL cells. 7 days later, 4×10^6 CAR-T cells were administered intravenously. Tumor burden was monitored by bioluminescence imaging using the IVIS Lumina system. Data are represented as mean ± SD (n = 3 for NTD and n = 7 for CAR5). (G) CAR-T cell kinetics in peripheral blood was analyzed in (F) by flow cytometry with Absolute Counting Beads. Data are represented as mean ± SD (n = 3 for NTD and n = 7 for CAR5). (H) Kaplan-Meier survival curves for mice described in (F). Statistical analyses were performed using one-way ANOVA with Tukey's multiple comparisons test for (F), a linear mixed-effects model with donor as a random effect followed by Tukey's test for (B–E and G), and log rank (Mantel-Cox) test for (H).

DISCUSSION

This study demonstrates that modulating antigen-binding affinity in CD5-specific CAR-T cells significantly influences fratricide, T cell exhaustion, and therapeutic efficacy. Importantly, low-affinity CD5 CAR-T cells exhibited reduced fratricidal activity and attenuated exhaustion, ultimately resulting in improved and sustained anti-tumor responses. These findings suggest that tuning CAR affinity may serve as a viable and gene editing-free alternative to

conventional strategies for optimizing CAR-T cell function.[31,32] Notably, although the intrinsic affinity difference between variants was only approximately 2-fold, this modest shift translated into distinct functional outcomes *in vivo*. While the high-affinity CAR-T cells eventually led to disease relapse driven by exhaustion, the low-affinity counterparts achieved durable complete remission. We attribute this substantial therapeutic divergence to the transition of monovalent affinity into multivalent functional avidity within the immunological synapse. Thus, our study provides a proof of concept that incremental affinity tuning is sufficient to optimize CD5 CAR-T cell efficacy.

To mechanistically dissect this relationship, we performed both site-directed and random mutagenesis to generate CAR variants with a broad range of binding affinities. These variants confirmed that antigen-binding strength directly regulates the extent of fratricide and exhaustion. Specifically, low-affinity CARs derived from the high-affinity A2 clone exhibited reduced T cell dysfunction, while high-affinity variants of the low-affinity C7 clone exhibited enhanced fratricide and exhaustion. These data underscore the pivotal role of affinity in shaping the phenotypic fate and therapeutic fitness of CAR-T cells.

In particular, low-affinity CD5 CAR-T cells exhibited minimal fratricide and expressed lower levels of exhaustion-associated markers, yet achieved superior long-term tumor control *in vivo*. This stands in stark contrast to high-affinity CARs, including the clinical-stage H65 clone utilized in the MAGENTA clinical trial (NCT03081910).[8] While recent clinical data confirmed the safety of H65-based CAR-T, the complete remission rate remained at approximately 22% (2/9 patients) in relapsed/refractory T cell lymphoma, highlighting a need for improved durability. By achieving durable remission in a stringent model where the H65 CAR5 showed limited efficacy, our findings demonstrate that affinity tuning significantly enhances *in vivo* persistence and efficacy compared to this high-affinity benchmark.

This striking discrepancy between potent *in vitro* cytotoxicity and limited *in vivo* persistence in high-affinity CARs, such as H65, is likely attributable to the duration and context of CAR stimulation. Short-term *in vitro* assays primarily measure acute cytotoxic responses associated with baseline activation, whereas prolonged antigen exposure *in vivo* results in sustained CAR signaling, leading to T cell exhaustion. These findings suggest that the temporal dynamics of antigen engagement critically influence CAR-T cell function and therapeutic outcomes and highlight the importance of aligning CAR affinity with the physiological context of T cell malignancies.

Importantly, the therapeutic benefits of affinity modulation were preserved in an allogeneic setting using γδ T cells. Owing to their lack of alloreactivity and reduced risk of GvHD, γδ T cells offer an attractive off-the-shelf platform for treating T cell malignancies.[33] We showed that γδ CAR-T cells incorporating low-affinity CD5 CARs exhibited diminished exhaustion and improved *in vivo* persistence compared to their high-affinity counterparts, translating to superior antitumor efficacy. These findings reinforce the generalizability of affinity tuning across CAR platforms and establish it as a broadly applicable design principle for next-generation cellular immunotherapies.

Prior studies have suggested that CARs with faster off-rates can limit prolonged immune synapse formation and excessive CAR signaling.[25,34] In this context, the relatively faster off-rate (higher K_{off}) of the C7 scFv might have contributed to preserving T cell functionality. Furthermore, we recognize that antigen downregulation represents a potential escape mechanism, particularly for low-affinity CAR-T cells that may require higher antigen density for activation. Conversely, however, excessively high affinity can also drive immune escape through trogocytosis, a process where CAR-T cells strip antigen from tumor cells, leading to reversible antigen loss.[27] By identifying an optimal affinity window, our strategy aims to minimize such antigen escape and subsequent immune evasion while maintaining sufficient potency. Future studies utilizing heterogeneous tumor models will be essential to validate this balance.

Despite these encouraging results, several limitations of our study warrant consideration. Our functional validations primarily utilized the Jurkat cell model, and the current lack of primary T cell or patient-derived xenograft models may limit the immediate translatability of these findings. Nevertheless, although the precise epitopes recognized by A2 and C7 were not formally mapped, the use of both clones across a broad range of binding affinities enabled us to interrogate the role of avidity in modulating fratricide and exhaustion. While epitope-dependent effects cannot be entirely ruled out, the consistency of phenotypic trends across multiple affinity variants within each scFv clone strengthens our conclusion that avidity is the dominant factor. Nevertheless, as epitope location is known to influence CAR signaling dynamics and immunological synapse formation,[35,36] future studies incorporating precise epitope mapping will be instrumental in further delineating the relative contributions of affinity and epitope specificity.

Looking forward, systematic mapping of optimal affinity ranges across diverse antigen-CAR pairings—including additional targets, costimulatory domains, and CAR architectures—will be essential to establish the generalizability of this strategy and may help define a "Goldilocks zone" that balances activation, persistence, and safety. Moreover, integrating affinity-tuned CARs with additional armoring strategies, such as the incorporation of cytokines or inhibitory modules, may further potentiate antitumor efficacy and functional persistence. Ultimately, incorporating these insights into clinically scalable CAR-T manufacturing platforms and evaluating their performance in translational and immune-competent models will be key steps toward advancing affinity-tuned CAR-T therapies into clinical application.

In conclusion, this study provides compelling evidence that antigen-binding affinity is a critical and tunable determinant of CAR-T cell

function. By modulating CAR affinity, we demonstrate an effective strategy to reduce fratricide and exhaustion while enhancing therapeutic efficacy, without the need for complex genetic manipulation. These findings offer a conceptual and practical framework for the development of next-generation CAR-T cells tailored for T cell malignancies, based on simplified and broadly applicable engineering principles.

MATERIALS AND METHODS

Screening for human CD5-specific antibody

Antibody screening and production were obtained from YntoAb, Inc. (Seongnam-si, Gyeonggi-do, Republic of Korea). During biopanning, a human phage display library (YntoAb, Republic of Korea) was used to generate anti-CD5 antibody. Briefly, recombinant human CD5 protein (ACROBiosystems, USA; Cat#CD5-H52H58) was immobilized as the target antigen and incubated with the scFv-displaying phages. Bound phages were recovered and amplified in *E. coli*, and the biopanning process was repeated for three rounds. Enriched phage clones were screened for CD5 binding by ELISA. CD5-specific binders were subcloned into scFv-Fc expression vectors and expressed in *E. coli*, and the resulting periplasmic extracts were incubated with CD5-expressing cell lines to identify clones with cell-surface CD5-binding activity.

To generate higher-affinity variants of the low-affinity C7 clone, random mutations were introduced into the heavy-chain CDR3 region and a mutant scFv phage library was constructed. CD5-binding clones were enriched through three additional rounds of biopanning, and their enriched scFv sequences were identified via next-generation sequencing. For affinity attenuation of the high-affinity A2 clone, alanine-scanning mutagenesis was performed by individually substituting each residue in the CDR-H3 with alanine. K562 cells expressing mutant scFv-based CAR were incubated with rhCD5, and clones with reduced binding compared to wild-type scFv-based CAR were selected.

Plasmid construction

To construct the lentiviral transfer plasmid encoding the CD5-specific CAR, each scFv (H65, A2, C7, F8, D9, C7-S6E, C7-S6E/S7E, A2-D1A, A2-W2A, and A2-Y4A) was fused to the Myc tag, the CD8α spacer and transmembrane domains, the 4-1BB (CD137) costimulatory domain, and the CD3ζ signaling domain and cloned into a lentiviral transfer plasmid.[37]

To construct the lentiviral transfer plasmid encoding the CD5 (CD5-P2A-eGFP), the human CD5 sequence (GenBank: NM_014207.4) was synthesized and then inserted between the EF1α promoter and the P2A sequence of the pLV-EF1α-P2A-eGFP plasmid. Lentiviral transfer plasmids encoding either ZsGreen or firefly luciferase-green fluorescent protein (ffluc/GFP; GL) were constructed by synthesizing and inserting between the EF1α promoter and the WPRE element of the lentiviral vector.

Antibody affinity measurement

All scFv-binding affinity measurements were conducted at Y-Biologics (Republic of Korea). The sequences of anti-CD5 scFvs were cloned into an N293F expression vector containing an mIgG2a Fc tag. Each plasmid was transfected into HEK293F cells, and recombinant scFv proteins were purified using size-exclusion chromatography. Binding kinetics was measured using the Octet RH96 (Sartorius, Germany) according to the manufacturer's instructions. Briefly, recombinant anti-CD5 scFv-mIgG2a Fc fusion proteins were immobilized onto anti-mouse IgG Fc capture biosensors as ligands and binding was assessed using recombinant human CD5 extracellular domain protein (ACROBiosystems, USA; catalog no. CD5-H52H58) as analyte. Data were analyzed using Octet BLI Analysis Software v.12.2.

Cell lines and culture conditions

Jurkat, Nalm-6, Raji, K562, RPMI8402, CCRF-CEM, and HEK293T cells were purchased from the American Type Culture Collection (ATCC). HUT78, H9, HH, MJ cells were generously provided by Prof. Won Seok Kim (Samsung Medical Center, Seoul, Republic of Korea). K562 cells were transduced with lentiviral vectors encoding anti-CD5 CARs to generate K562 cells stably expressing individual CAR constructs. Jurkat cells were transduced to express GFP-Fluc (GL) or ZsGreen to generate Jurkat-GL and Jurkat-ZsGreen cells. Nalm-6 cells were transduced to express human CD5 (GenBank: NM_014207.3) generating Nalm-6-CD5 cells. HUT78, RPMI8402, and CCRF-CEM cells were transduced to express ZsGreen, generating HUT78-ZsGreen, RPMI8402-ZsGreen, and CCRF-CEM-ZsGreen cells, respectively. Jurkat, Nalm-6, Raji, K562, RPMI8402, and CCRF-CEM cells were cultured in RPMI-1640 medium (Gibco, USA) supplemented with 10% heat-inactivated fetal bovine serum (FBS, Gibco, USA), 2 mM L-glutamine (Gibco, USA), 0.1 mM non-essential amino acids (Gibco, USA), 1 mM sodium pyruvate (Gibco, USA), and 1% penicillin/streptomycin (Gibco, USA) in a humidified incubator with a 5% CO_2 at 37°C. HEK293T cells were cultured in Dulbecco's modified Eagle's medium (DMEM, Gibco, USA) supplemented with 10% heat-inactivated FBS, 2 mM L-glutamine, 0.1 mM non-essential amino acids, 1 mM sodium pyruvate, and 1% penicillin/streptomycin.

Generation of human CAR-T cells

Peripheral blood mononuclear cells (PBMCs) were obtained from healthy adult donors at the Seoul National University Hospital (SNUH, Seoul, Republic of Korea).

HEK293T cells were seeded at 7×10^6 cells per 100-mm dish coated with poly-D-lysine, 2 days prior to transduction. After 24 h, cells were co-transfected with 5.35 μg lentiviral transfer plasmid, 0.93 μg pCURO-ENV3 (VSV-G envelope), 2.06 μg pCURO-PKG6 (Rev), and 2.06 μg pCURO-PKG3 (Gag/Pol), using jetOPTIMUS (Polyplus-transfection, France) according to the manufacturer's instructions. Lentiviral supernatants were harvested 24 h post-transfection, removed of cell debris by centrifugation at 1,600 rpm for 5 min, and immediately used to transduce T cells.

For αβ CAR-T cells, $CD4^+$ or $CD8^+$ T cells were positively selected from PBMCs using a MACS sorting system (Miltenyi Biotec, Germany; catalog no. 130-091-051) and activated for 48 h with TransAct (Miltenyi Biotec, Germany). For γδ CAR-T cells, αβ TCR^+ cells were depleted from PBMCs using MACS to enrich γδ T cells (Miltenyi Biotec, Germany; catalog no. 130-091-051). The enriched γδ T cells were activated for 48 h with 5 μM zoledronate (Samyang Biopharm, Republic of Korea) and 1,000 IU/mL interleukin (IL)-2 (BMI Korea, Republic of Korea).

For αβ CAR-T cell culture, cells were maintained in AIM-V medium (Gibco, USA) supplemented with 5% Immune Cell SR (Gibco, USA), 100 IU/mL recombinant human IL-2 (BMI Korea, Republic of Korea), and 1% penicillin/streptomycin (Gibco, USA). For γδ CAR-T cell culture, 4Cell Nutri-T GMP Medium (Sartorius, Germany) supplemented with 5% Immune Cell SR, 100 IU/mL IL-2, and 1% penicillin/streptomycin was used as the γδ T cell culture medium.

Activated αβ and γδ T cells were transduced with lentiviral supernatants in the presence of 12 μg/mL protamine sulfate (Sigma-Aldrich, USA). For αβ T cells, transduction was performed once via centrifugation at 1,000 × *g* for 90 min at 32°C, followed by incubation at 37°C. The next day was designated as day 0. For γδ T cells, transduction was performed twice: the first via centrifugation at 1,000 × *g* for 30 min at 32°C, followed by a second transduction 24 h later. The day after the second transduction was designated as day 0. Following transduction, both αβ and γδ T cells were cultured in their respective culture media supplemented with 100 IU/mL IL-2. Fresh culture medium was added on days 3 and 7.

Flow cytometry

Flow cytometry was performed on a FACSVerse instrument (BD Biosciences, USA), and data were analyzed with FlowJo software (Tree Star, USA). For surface staining, 2×10^5 cells were stained with fluorophore-conjugated antibodies diluted in 100 μL of fluorescence-activated cell sorting (FACS) buffer (1% BSA in DPBS) for 15 min at 25°C in the dark. Cells were washed with 2 mL of FACS buffer, resuspended, and analyzed. For intracellular staining of TOX, 5×10^5 cells were fixed and permeabilized using 1 mL of Fixation/Permeabilization solution (Miltenyi Biotec, Germany) for 30 min at 4°C, washed with 2 mL of Permeabilization buffer, and then stained with the appropriate antibody. CAR expression was detected using either AF647-conjugated anti-Myc-tag antibody (clone 9B11, Cell Signaling Technology) or biotinylated recombinant human CD5 (ACROBiosystems, USA) followed by AF647-conjugated streptavidin (BioLegend, USA). For detection of cell surface-bound anti-CD5 recombinant scFv, 2×10^5 cells were incubated with 10 ng of mIgG2a-Fc-tagged anti-CD5 scFv protein (Y-Biologics, Republic of Korea), washed, and subsequently stained with AF647-conjugated anti-mIgG2a antibody (clone RMG2a-62, BioLegend). The following antibodies were used: BioLegend, CD5-PE (clone UCHT2), CD69-PE (clone FN50), LAG3-FITC (Clone 7H2C65), mIgG2a-AF647 (clone RMG2a-62), and streptavidin-AF647; BD Biosciences, CD4-V500 (clone RPA-T4), CD8-V450 (clone RPA-T8), αβ TCR-PE (clone IP26), and γδ TCR-BV421 (clone 11F2); Thermo Fisher Scientific, PD-1-PE (clone J105) and CD27-PE (clone O323); Miltenyi Biotec, TOX-APC (clone REA473), Vδ1-PE-Cy7 (clone REA173), and Vδ2-V500 (clone 123R3); Cell Signaling Technology, Myc-AF647 or PE (clone 9B11).

Repeated antigen stimulation

3×10^5 CAR-T cells were co-cultured with Jurkat cells at a 3:1 E:T ratio (defined as co-culture day 0). Thereafter, 1×10^5 Jurkat cells were added twice weekly from co-culture day 3. On days 7, 14, 21, and 28, absolute numbers of CAR-T cells were quantified using anti-Myc-tag antibody staining and CountBright Absolute Counting Beads (Thermo Fisher Scientific, USA) according to the manufacturer's instructions. Changes in CAR-T cell numbers over time were calculated by dividing the absolute counts on days 14, 21, and 28 by the count measured on day 7. Absolute numbers of Jurkat cells were quantified based on the CAR-negative cell population on days 0, 7, 14, 21, and 28.

Cytotoxicity assay

To evaluate the cytotoxic activity of CAR-T cells, 1×10^4 target cells were co-cultured with CAR-T cells at 10:1, 3:1, or 1:1 E:T ratios in 200 μL of complete T cell medium without IL-2 in 96-well flat-bottom plates for up to 72 h. Each condition was tested in triplicate wells. GFP fluorescence intensity was measured every 4 h using the IncuCyte S3 Live-Cell Analysis System (Sartorius, Germany). Total integrated GFP intensity per well was used as a quantitative measure of viable target cells. Values of total integrated GFP intensity were normalized to the GFP intensity of the starting point.

In vivo xenograft models

All animal procedures were approved by the Institutional Animal Care and Use Committee (IACUC) of Curocell, Inc. and conducted in accordance with national and institutional guidelines. NOG mice (6–8 weeks old) were purchased from KOATECH (Republic of Korea). Mice were intravenously injected via the tail vein with 1×10^6 Jurkat-GL cells, followed 7 days later by tail vein injection of the indicated dose of CAR-T cells. Tumor burden was assessed by bioluminescence imaging following intraperitoneal injection of luciferin (PerkinElmer, USA) according to the manufacturer's instructions, using the IVIS Lumina X5 imaging system (PerkinElmer, USA). Bioluminescence signals were quantified using the Living Image software (PerkinElmer, USA). Tumor growth was monitored weekly. Absolute counts of CAR-T cells in peripheral blood were determined on days 0, 3, 7, 15, and 21 post-infusion using CountBright Absolute Counting Beads (Thermo Fisher Scientific, USA) according to the manufacturer's instructions.

Quantitation of cytokine levels

Culture supernatants were collected on days 3, 7, and 10 during CAR-T cell expansion and stored at −80°C. In a separate experiment, supernatants were harvested 72 h after *in vitro* cytotoxicity assays and stored at −80°C. Cytokine levels of IFN-γ and TNF-α in supernatant were quantified by cytometric bead array using the CBA

Human Soluble Protein Master Buffer Kit, Human IFN-γ Flex Set and Human TNF-α Flex Set (BD Bioscience, USA) according to the manufacturer's instructions.

Statistical analysis

Statistical analyses were performed using GraphPad Prism 10 (GraphPad Software, Inc., USA) and R (v.4.5.2; R Foundation for Statistical Computing, Austria) with RStudio (Posit Software, Inc., USA). For experiments consisting of technical replicates only, statistical comparisons were conducted using one-way ANOVA. For experiments performed with multiple donors, group comparisons were assessed using a linear mixed-effects model with CAR construct as a fixed effect and donor as a random effect (random intercept). Post hoc multiple comparisons were performed using Tukey's test. Survival curves were estimated using the Kaplan-Meier method, and statistical significance was assessed using the log rank (Mantel-Cox) test. A p value <0.05 was considered statistically significant.

DATA AND CODE AVAILABILITY

All data are available upon request from authors.

ACKNOWLEDGMENTS

This work was supported by Curocell Inc.

AUTHOR CONTRIBUTIONS

Y.-H.L., J.-H.J., H.J.C., and Y.R.S. designed the experiments and wrote the manuscript. J.H.J., H.J.C., H.B.L., S.R.Y., and H.J.L. performed the experiments and analyzed the data. Y.-H.L. and H.C.K. analyzed the data and wrote the manuscript.

DECLARATION OF INTERESTS

Y.-H.L., J.-H.J., Y.R.S., S.R.Y., H.B.L., H.J.L., H.J.C., and H.C.K. are employees at Curocell Inc.

SUPPLEMENTAL INFORMATION

Supplemental information can be found online at https://doi.org/10.1016/j.omton.2026.201158.

REFERENCES

1. Wei, W., Yang, D., Chen, X., Liang, D., Zou, L., and Zhao, X. (2022). Chimeric antigen receptor T-cell therapy for T-ALL and AML. Front. Oncol. *12*, 967754. https://doi.org/10.3389/fonc.2022.967754.
2. Luan, Y., Li, X., Luan, Y., Luo, J., Dong, Q., Ye, S., Li, Y., Li, Y., Jia, L., Yang, J., and Yang, D.H. (2024). Therapeutic challenges in peripheral T-cell lymphoma. Mol. Cancer *23*, 2. https://doi.org/10.1186/s12943-023-01904-w.
3. Ureshino, H., Kamachi, K., and Kimura, S. (2019). Mogamulizumab for the Treatment of Adult T-cell Leukemia/Lymphoma. Clin. Lymphoma Myeloma Leuk. *19*, 326–331. https://doi.org/10.1016/j.clml.2019.03.004.
4. Begna, K.H., Abdallah, N.H., Janania-Martinez, M., Mangaonkar, A.A., Rangan, A., Herrick, J.L., and Gangat, N. (2024). Daratumumab and brentuximab vedotin combination therapy in T-cell acute lymphoblastic leukemia refractory to conventional chemotherapy and allogeneic stem cell transplant. Haematologica *109*, 689–692. https://doi.org/10.3324/haematol.2023.283740.
5. Horwitz, S., O'Connor, O.A., Pro, B., Illidge, T., Fanale, M., Advani, R., Bartlett, N.L., Christensen, J.H., Morschhauser, F., Domingo-Domenech, E., et al. (2019). Brentuximab vedotin with chemotherapy for CD30-positive peripheral T-cell lymphoma (ECHELON-2): a global, double-blind, randomised, phase 3 trial. Lancet Lond. Engl. *393*, 229–240. https://doi.org/10.1016/S0140-6736(18)32984-2.
6. Kim, Y.H., Bagot, M., Pinter-Brown, L., Rook, A.H., Porcu, P., Horwitz, S.M., Whittaker, S., Tokura, Y., Vermeer, M., Zinzani, P.L., et al. (2018). Mogamulizumab versus vorinostat in previously treated cutaneous T-cell lymphoma (MAVORIC): an international, open-label, randomised, controlled phase 3 trial. Lancet Oncol. *19*, 1192–1204. https://doi.org/10.1016/S1470-2045(18)30379-6.
7. Mamonkin, M., Rouce, R.H., Tashiro, H., and Brenner, M.K. (2015). A T-cell-directed chimeric antigen receptor for the selective treatment of T-cell malignancies. Blood *126*, 983–992. https://doi.org/10.1182/blood-2015-02-629527.
8. Hill, L.C., Rouce, R.H., Wu, M.J., Wang, T., Ma, R., Zhang, H., Mehta, B., Lapteva, N., Mei, Z., Smith, T.S., et al. (2024). Antitumor efficacy and safety of unedited autologous CD5.CAR T cells in relapsed/refractory mature T-cell lymphomas. Blood *143*, 1231–1241. https://doi.org/10.1182/blood.2023022204.
9. Alcantara, M., Tesio, M., June, C.H., and Houot, R. (2018). CAR T-cells for T-cell malignancies: challenges in distinguishing between therapeutic, normal, and neoplastic T-cells. Leukemia *32*, 2307–2315. https://doi.org/10.1038/s41375-018-0285-8.
10. Ren, A., Tong, X., Xu, N., Zhang, T., Zhou, F., and Zhu, H. (2023). CAR T-Cell Immunotherapy Treating T-ALL: Challenges and Opportunities. Vaccines *11*, 165. https://doi.org/10.3390/vaccines11010165.
11. Maciocia, N., Wade, B., and Maciocia, P. (2025). CAR T-cell therapies for T-cell malignancies: does cellular immunotherapy represent the best chance of cure? Blood Adv. *9*, 913–923. https://doi.org/10.1182/bloodadvances.2023012263.
12. Gomes-Silva, D., Srinivasan, M., Sharma, S., Lee, C.M., Wagner, D.L., Davis, T.H., Rouce, R.H., Bao, G., Brenner, M.K., and Mamonkin, M. (2017). CD7-edited T cells expressing a CD7-specific CAR for the therapy of T-cell malignancies. Blood *130*, 285–296. https://doi.org/10.1182/blood-2017-01-761320.
13. Alvarez-Fernández, C., Escribà-Garcia, L., Caballero, A.C., Escudero-López, E., Ujaldón-Miró, C., Montserrat-Torres, R., Pujol-Fernández, P., Sierra, J., and Briones, J. (2021). Memory stem T cells modified with a redesigned CD30-chimeric antigen receptor show an enhanced antitumor effect in Hodgkin lymphoma. Clin. Transl. Immunol. *10*, e1268. https://doi.org/10.1002/cti2.1268.
14. Cooper, M.L., Choi, J., Staser, K., Ritchey, J.K., Devenport, J.M., Eckardt, K., Rettig, M.P., Wang, B., Eissenberg, L.G., Ghobadi, A., et al. (2018). An "off-the-shelf" fratricide-resistant CAR-T for the treatment of T cell hematologic malignancies. Leukemia *32*, 1970–1983. https://doi.org/10.1038/s41375-018-0065-5.
15. Raikar, S.S., Fleischer, L.C., Moot, R., Fedanov, A., Paik, N.Y., Knight, K.A., Doering, C.B., and Spencer, H.T. (2018). Development of chimeric antigen receptors targeting T-cell malignancies using two structurally different anti-CD5 antigen binding domains in NK and CRISPR-edited T cell lines. OncoImmunology *7*, e1407898. https://doi.org/10.1080/2162402X.2017.1407898.
16. Dai, Z., Mu, W., Zhao, Y., Cheng, J., Lin, H., Ouyang, K., Jia, X., Liu, J., Wei, Q., Wang, M., et al. (2022). T cells expressing CD5/CD7 bispecific chimeric antigen receptors with fully human heavy-chain-only domains mitigate tumor antigen escape. Signal Transduct. Target. Ther. *7*, 85. https://doi.org/10.1038/s41392-022-00898-z.
17. Ma, R., Woods, M., Burkhardt, P., Crooks, N., van Leeuwen, D.G., Shmidt, D., Couturier, J., Chaumette, A., Popat, D., Hill, L.C., et al. (2024). Chimeric antigen receptor-induced antigen loss protects CD5.CART cells from fratricide without compromising on-target cytotoxicity. Cell Rep. Med. *5*, 101628. https://doi.org/10.1016/j.xcrm.2024.101628.
18. Tsuchida, C.A., Brandes, N., Bueno, R., Trinidad, M., Mazumder, T., Yu, B., Hwang, B., Chang, C., Liu, J., Sun, Y., et al. (2023). Mitigation of chromosome loss in clinical CRISPR-Cas9-engineered T cells. Cell *186*, 4567–4582.e20. https://doi.org/10.1016/j.cell.2023.08.041.
19. Chen, X., Zhong, S., Zhan, Y., and Zhang, X. (2024). CRISPR-Cas9 applications in T cells and adoptive T cell therapies. Cell. Mol. Biol. Lett. *29*, 52. https://doi.org/10.1186/s11658-024-00561-1.
20. Hwang, G.-H., Lee, S.-H., Oh, M., Kim, S., Habib, O., Jang, H.-K., Kim, H.S., Kim, Y., Kim, C.H., Kim, S., and Bae, S. (2025). Large DNA deletions occur during DNA repair at 20-fold lower frequency for base editors and prime editors than for Cas9 nucleases. Nat. Biomed. Eng. *9*, 79–92. https://doi.org/10.1038/s41551-024-01277-5.
21. Chiesa, R., Georgiadis, C., Syed, F., Zhan, H., Etuk, A., Gkazi, S.A., Preece, R., Ottaviano, G., Braybrook, T., Chu, J., et al. (2023). Base-Edited CAR7 T Cells for

Relapsed T-Cell Acute Lymphoblastic Leukemia. N. Engl. J. Med. *389*, 899–910. https://doi.org/10.1056/NEJMoa2300709.

22. Hudecek, M., Lupo-Stanghellini, M.-T., Kosasih, P.L., Sommermeyer, D., Jensen, M.C., Rader, C., and Riddell, S.R. (2013). Receptor affinity and extracellular domain modifications affect tumor recognition by ROR1-specific chimeric antigen receptor T cells. Clin. Cancer Res. *19*, 3153–3164. https://doi.org/10.1158/1078-0432.CCR-13-0330.

23. Richman, S.A., Nunez-Cruz, S., Moghimi, B., Li, L.Z., Gershenson, Z.T., Mourelatos, Z., Barrett, D.M., Grupp, S.A., and Milone, M.C. (2018). High-Affinity GD2-Specific CAR T Cells Induce Fatal Encephalitis in a Preclinical Neuroblastoma Model. Cancer Immunol. Res. *6*, 36–46. https://doi.org/10.1158/2326-6066.CIR-17-0211.

24. Ghorashian, S., Kramer, A.M., Onuoha, S., Wright, G., Bartram, J., Richardson, R., Albon, S.J., Casanovas-Company, J., Castro, F., Popova, B., et al. (2019). Enhanced CAR T cell expansion and prolonged persistence in pediatric patients with ALL treated with a low-affinity CD19 CAR. Nat. Med. *25*, 1408–1414. https://doi.org/10.1038/s41591-019-0549-5.

25. Mao, R., Kong, W., and He, Y. (2022). The affinity of antigen-binding domain on the antitumor efficacy of CAR T cells: Moderate is better. Front. Immunol. *13*, 1032403. https://doi.org/10.3389/fimmu.2022.1032403.

26. Boettcher, M., Joechner, A., Li, Z., Yang, S.F., and Schlegel, P. (2022). Development of CAR T Cell Therapy in Children-A Comprehensive Overview. J. Clin. Med. *11*, 2158. https://doi.org/10.3390/jcm11082158.

27. Olson, M.L., Mause, E.R.V., Radhakrishnan, S.V., Brody, J.D., Rapoport, A.P., Welm, A.L., Atanackovic, D., and Luetkens, T. (2022). Low-affinity CAR T cells exhibit reduced trogocytosis, preventing rapid antigen loss, and increasing CAR T cell expansion. Leukemia *36*, 1943–1946. https://doi.org/10.1038/s41375-022-01585-2.

28. Vander Mause, E.R., Baker, J.M., Dietze, K.A., Radhakrishnan, S.V., Iraguha, T., Omili, D., Davis, P., Chidester, S.L., Modzelewska, K., Panse, J., et al. (2023). Systematic single amino acid affinity tuning of CD229 CAR T cells retains efficacy against multiple myeloma and eliminates on-target off-tumor toxicity. Sci. Transl. Med. *15*, eadd7900. https://doi.org/10.1126/scitranslmed.add7900.

29. Fonseca, S., Pereira, V., Lau, C., Teixeira, M.D.A., Bini-Antunes, M., and Lima, M. (2020). Human Peripheral Blood Gamma Delta T Cells: Report on a Series of Healthy Caucasian Portuguese Adults and Comprehensive Review of the Literature. Cells *9*, 729. https://doi.org/10.3390/cells9030729.

30. Spour, E.F., Leemhuis, T., Jenski, L., Redmond, R., Fillak, D., and Jansen, J. (1990). Characterization of normal human CD3+ CD5- and gamma delta T cell receptor positive T lymphocytes. Clin. Exp. Immunol. *80*, 114–121. https://doi.org/10.1111/j.1365-2249.1990.tb06450.x.

31. Patel, R.P., Ghilardi, G., Zhang, Y., Chiang, Y.-H., Xie, W., Guruprasad, P., Kim, K.H., Chun, I., Angelos, M.G., Pajarillo, R., et al. (2024). CD5 deletion enhances the antitumor activity of adoptive T cell therapies. Sci. Immunol. *9*, eadn6509. https://doi.org/10.1126/sciimmunol.adn6509.

32. Chun, I., Kim, K.H., Chiang, Y.-H., Xie, W., Lee, Y.G.G., Pajarillo, R., Rotolo, A., Shestova, O., Hong, S.J., Abdel-Mohsen, M., et al. (2020). CRISPR-Cas9 Knock out of CD5 Enhances the Anti-Tumor Activity of Chimeric Antigen Receptor T Cells. Blood *136*, 51–52. https://doi.org/10.1182/blood-2020-136860.

33. Ganapathy, T., Radhakrishnan, R., Sakshi, S., and Martin, S. (2023). CAR γδ T cells for cancer immunotherapy. Is the field more yellow than green? Cancer Immunol. Immunother. *72*, 277–286. https://doi.org/10.1007/s00262-022-03260-y.

34. Srivastava, S., and Riddell, S.R. (2015). Engineering CAR-T cells: Design concepts. Trends Immunol. *36*, 494–502. https://doi.org/10.1016/j.it.2015.06.004.

35. Hombach, A.A., Schildgen, V., Heuser, C., Finnern, R., Gilham, D.E., and Abken, H. (2007). T cell activation by antibody-like immunoreceptors: the position of the binding epitope within the target molecule determines the efficiency of activation of redirected T cells. J. Immunol. *178*, 4650–4657. https://doi.org/10.4049/jimmunol.178.7.4650.

36. Chang, Z.L., and Chen, Y.Y. (2017). CARs: Synthetic Immunoreceptors for Cancer Therapy and Beyond. Trends Mol. Med. *23*, 430–450. https://doi.org/10.1016/j.molmed.2017.03.002.

37. Lee, Y.-H., Lee, H.J., Kim, H.C., Lee, Y., Nam, S.K., Hupperetz, C., Ma, J.S.Y., Wang, X., Singer, O., Kim, W.S., et al. (2022). PD-1 and TIGIT downregulation distinctly affect the effector and early memory phenotypes of CD19-targeting CAR T cells. Mol. Ther. *30*, 579–592. https://doi.org/10.1016/j.ymthe.2021.10.004.